Nuclear Instruments and Methods in Physics Research B 554 (2024) 165460

Contents lists available at ScienceDirect

Nuclear Inst. and Methods in Physics Research, B

journal homepage: www.elsevier.com/locate/nimb

Full Length Article

Measurement of cross-section of the ^{6}Li(d,α)^{4}He, ^{6}Li(d,p)^{7}Li, ^{6}Li(d,p)^{7}Li*, ^{7}Li(d,α)^{5}He, and ^{7}Li(d,nα)^{4}He reactions at the deuteron energies from 0.3 MeV to 2.2 MeV

Sergey Taskaev [a,b,c,*], Marina Bikchurina [a,b], Timofey Bykov [a,b], Dmitrii Kasatov [a,b], Iaroslav Kolesnikov [a,b], Georgii Ostreinov [a,b], Sergey Savinov [a,b], Evgeniia Sokolova [a,b]

[a] Budker Institute of Nuclear Physics, 11 Lavrentiev Ave., 630090 Novosibirsk, Russia
[b] Novosibirsk State University, 2 Pirogov Str., 630090 Novosibirsk, Russia
[c] Joint Institute for Nuclear Research, 6 Joliot-Curie Str., 141980 Dubna, Russia

ARTICLE INFO

Keywords:
Cross-section
Deuteron beam
Lithium target

ABSTRACT

The interaction of a deuteron beam with lithium is characterized by a high yield of neutrons, high energy of neutrons and a large variety of reactions. The reliable data of the reactions cross-sections are important for many applications, including radiation testing of advanced materials and equipment. The experimental data on the cross-sections differ greatly from one author to another; for a number of reactions there is no data on the cross-section in the databases. Measurements of the reactions cross-sections were carried out at the accelerator-based neutron source VITA at Budker Institute of Nuclear Physics (Novosibirsk, Russia) using an α-spectrometer. The ^{6}Li(d,α)^{4}He, ^{6}Li(d,p)^{7}Li, ^{6}Li(d,p)^{7}Li*, ^{7}Li(d,α)^{5}He, and ^{7}Li(d,nα)^{4}He reactions cross-sections at deuteron energies from 0.3 MeV to 2.2 MeV have been measured. The obtained data are presented tabular form.

1. Introduction

Intense fast neutron fluxes are required for many applications, including radiation testing of advanced materials and equipment. The highest neutron yield is provided by the Li(d,n) reaction starting with the energy of 1 MeV [1]. There are ten reactions when a deuteron interacts with a lithium nucleus, five of which lead to the generation of neutrons. This interaction results in the production of neutrons, protons, tritium, ^{3}He, α-particles, ^{7}Li, and ^{7}Be [2]. The reaction cross-section values are certainly important for nuclear data evaluation, for estimating the neutron spectrum in radiation testing of materials, and for considering the possibility of using lithium as the first wall of a fusion reactor. However, the data on cross-sections in the literature and databases differ significantly [3–12]; for a number of reactions there are no data on the cross-section. Differences in the data from different authors are most likely due to the difficulty of determining the thickness of lithium layer due to its high chemical reactivity, which does not allow the use of some measurement methods.

The aim of this work is to measure cross-sections of the ^{6}Li(d,α)^{4}He, ^{6}Li(d,p)^{7}Li, ^{6}Li(d,p)^{7}Li*, ^{7}Li(d,α)^{5}He, and ^{7}Li(d,nα)^{4}He reactions.

2. Experimental facility

The study was carried out at the accelerator-based neutron source VITA at Budker Institute of Nuclear Physics in Novosibirsk, Russia [13,14]. The layout of the experimental facility is shown in Fig. 1.

The DC vacuum insulated tandem accelerator *1* is used to provide a deuteron beam and to direct it to a lithium target *4* through a 1 mm collimator *3*. The deuteron beam has the diameter of 5 mm on the surface of the lithium target. The deuteron beam energy can vary within the range of 0.3–2.2 MeV, keeping the high-energy stability of 0.1 %. The beam current can also vary in a wide range (from 0.5 mA to 10 mA) with the high current stability (0.4 %).

The deuteron beam current is measured and controlled by a non-destructive DC current transformer NPCT (Bergoz Instrumentation, France) *2* and by a calibrated resistance connected to the target assembly, which is electrically isolated from the facility. Although the target assembly is made in the form of a deep Faraday cup, there is electron emission from it at a level of 1 % of the ion current. Such electron emission increases the ion current by 1 %, and this fact is taken into account.

* Corresponding author at: 11 Lavrentiev Ave., 630090 Novosibirsk, Russia.
E-mail address: taskaev@inp.nsk.su (S. Taskaev).

https://doi.org/10.1016/j.nimb.2024.165460
Received 20 January 2024; Received in revised form 30 May 2024; Accepted 4 July 2024
Available online 8 July 2024

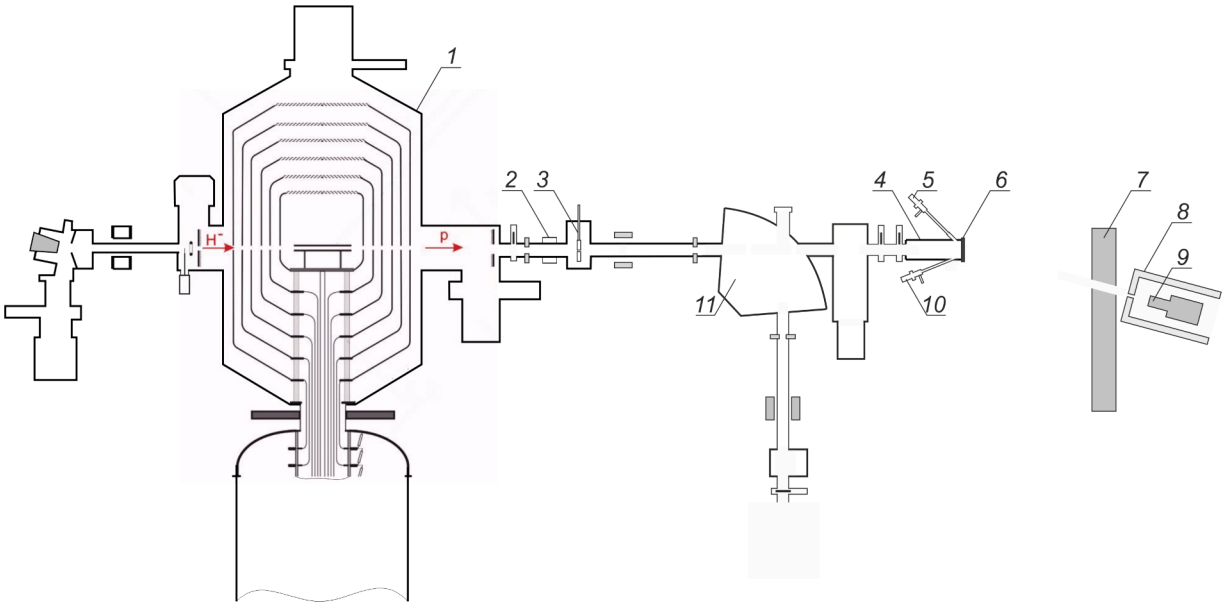

Fig. 1. Scheme of the experimental facility: *1* – vacuum insulated tandem accelerator, *2* – non-destructive DC current transformer, *3* – collimator, *4* – target assembly, 5 – α-spectrometer at 135°, 6 – lithium target, *7* – temporary concrete wall, *8* – lead collimator, *9* – γ-ray spectrometer, *10* – α-spectrometer at 168°, *11* – bending magnet.

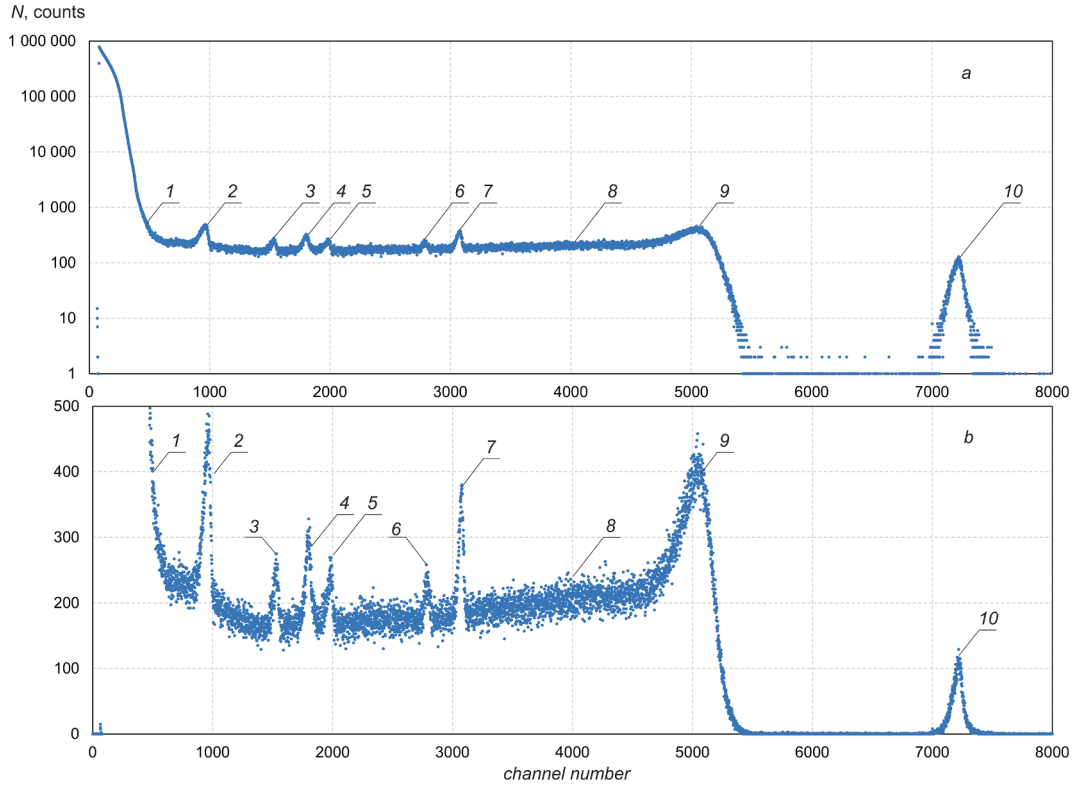

Fig. 2. The signal from the α-spectrometer at 0.6 MeV deuteron beam: *1* – back scattered deuterons, *2* – $^{16}O(d,p_1)^{17}O^*$ reaction protons, *3* – $^{16}O(d,p_0)^{17}O$ reaction protons, *4* – $^{16}O(d,\alpha)^{14}N$ reaction α-particles, *5* – $^{12}C(d,p_0)^{13}C$ reaction protons, *6* – $^{6}Li(d,p_1)^{7}Li^*$ reaction protons, *7* – $^{6}Li(d,p_0)^{7}Li$ reaction protons, *8* – $^{7}Li(d,n\alpha)^{4}He$ reaction α-particles, *9* – $^{7}Li(d,\alpha)^{5}He$ reaction α-particles, *10* – $^{6}Li(d,\alpha)^{4}He$ reaction α-particles.

Vacuum evaporation of lithium on the target was carried out at a separate stand. After the lithium deposition, closed with a gate valve to maintain vacuum inside the target assembly *4* was disconnected from the lithium evaporation stand, transferred to the experimental facility, and connected to the horizontal beam line. We evaporated natural lithium produced by the Novosibirsk Chemical Concentrates Plant; the used batch contained 99.956 % of lithium. The percentage of lithium-7 in natural lithium varies from 92.41 % [15] to 92.58 % [16]; we will assume the lithium-7 content is equal to the average value, namely 92.5 %.

The thickness of a lithium layer was measured by new *in situ* method [17]. The method is based on comparing the yield of 478 keV photons in

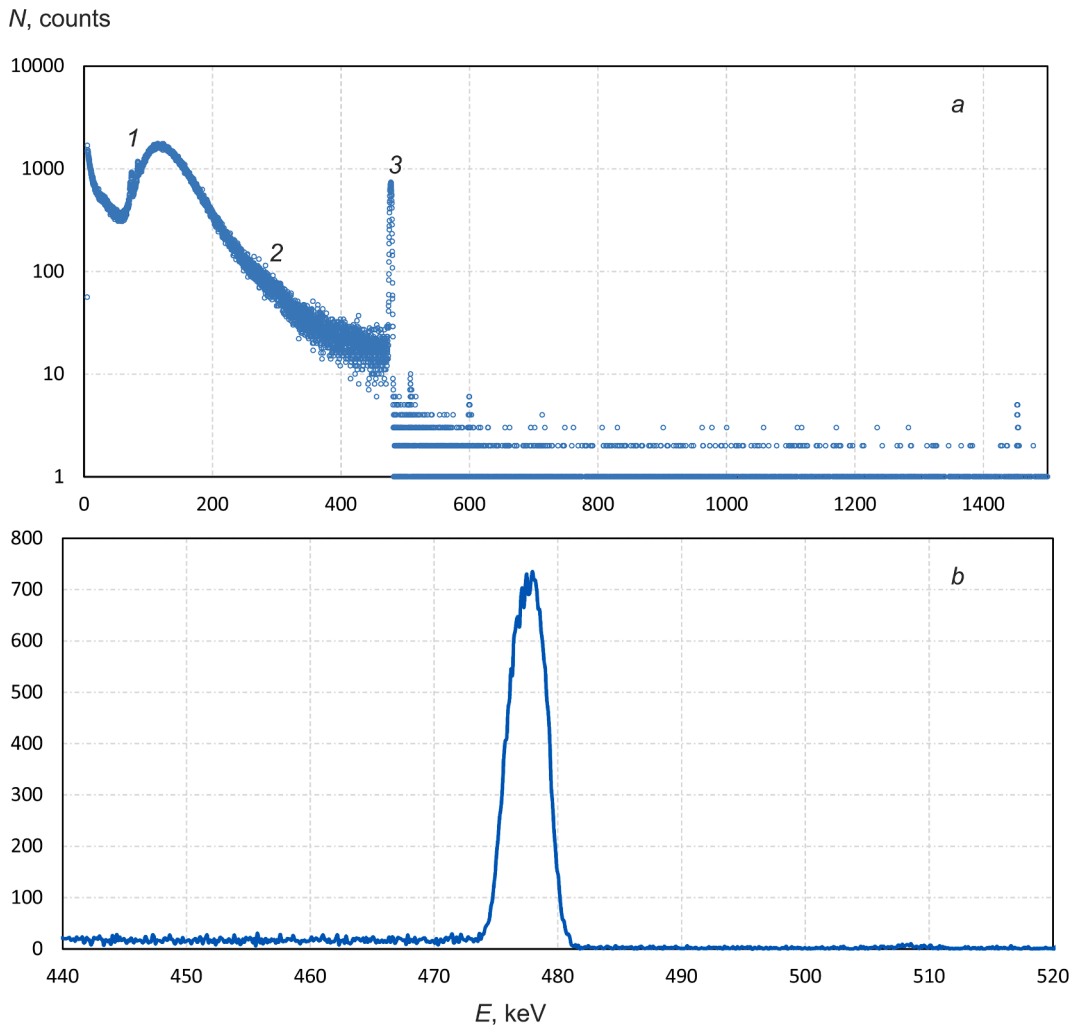

Fig. 3. The signal from HPGe γ-ray spectrometer when irradiating the thick lithium target: *1* – characteristic X-rays emitted by lead, *2* – bremsstrahlung of the accelerator, 3 – 478 keV photons emitted in the ^{7}Li(p,p'γ)^{7}Li reaction.

the ^{7}Li(p,p′γ)^{7}Li reaction from the investigated lithium layer and from a thick one irradiated by protons. The intensity of γ-radiation is measured by a high purity germanium γ-ray spectrometer SEG-1KP-IPTP 12 (Institute of Physical and Technical Problems, Dubna, Russia) *9*. To reduce the background signal the HPGe γ-ray spectrometer is placed in a lead collimator *8* with external diameter of 270 mm, 500 mm length and 50 mm wall thickness. Apart from the collimator, a 23 cm thick wall *7* built of concrete blocks protects the spectrometer from a bremsstrahlung of the accelerator.

The intensity and energy of charged particles (reaction products) were measured by an α-spectrometer (*5* and *10* in Fig. 1) with silicon semiconductor detector PDPA-1 K (Institute of Physical and Technical Problems, Dubna, Russia). Sensitive surface area of the detector was S = 20 mm^2, energy resolution 13 keV, energy equivalent of noise 7 keV, capacity 30 pF, entrance window thickness 0.08 μm, standard natural background in the range of 3–8 MeV 0.15 imp/cm^{2}h. The α-spectrometer was calibrated with two standard radiation sources based on the plutonium-239 radionuclide with activities of $4.01{\cdot}10^5$ Bq (passport No. 6887, marking 7165, 2P9-405.85, issue date 12.09.1985) and $1.21{\cdot}10^5$ Bq (passport No. 6882, marking 7160 1P9-105.85, issue date 12.09.1985). The confidence interval of each source activity measurement total error is equal of 19 % according to the passport. To determine the detection efficiency k of the α-spectrometer, the reference radiation sources were placed at the distance of 102.8 mm from the detector surface, and the activities were measured. The measured activities of the sources amounted to $4.16{\cdot}10^5$ Bq and $1.22{\cdot}10^5$ Bq, which is 4 % and 1.5 % higher than the passport ones; they corresponded to passport values within the margin of error. Since the measured values of the source activity correspond to the passport ones, we considered the detection efficiency of α-particles by the detector to be 100 %, i.e. $k = 1$ with an accuracy of 3 %.

The energy calibration of the spectrometer was carried out with an exemplary spectrometric α-source with the ^{226}Ra isotope (passport No. 425/331/10692-A, 21.10.1977) with the activity of $3.84{\cdot}10^4$ Bq, characterized by following energies of α-particles: 4748, 5453, 5966 and 7651 keV. It was established that the dependence of the energy E on a channel number N was linear and was described by the expression E [keV] = $1.3941{\cdot}N + 82.003$.

The measurements were carried out with two options for placing the α-spectrometer; in Fig. 1 they are shown as *5* and *10*. At the position 5 the α-spectrometer is placed at the angle of 135° at the distance of 722 mm from the place of generation of charged particles from lithium; at the position *10* the α-spectrometer is placed at the angle of 168° at the distance of 712 mm.

3. Reactions

When a deuteron with the energy of less than 2.2 MeV interacts with a lithium nucleus, the following nuclear reactions occur [2]:

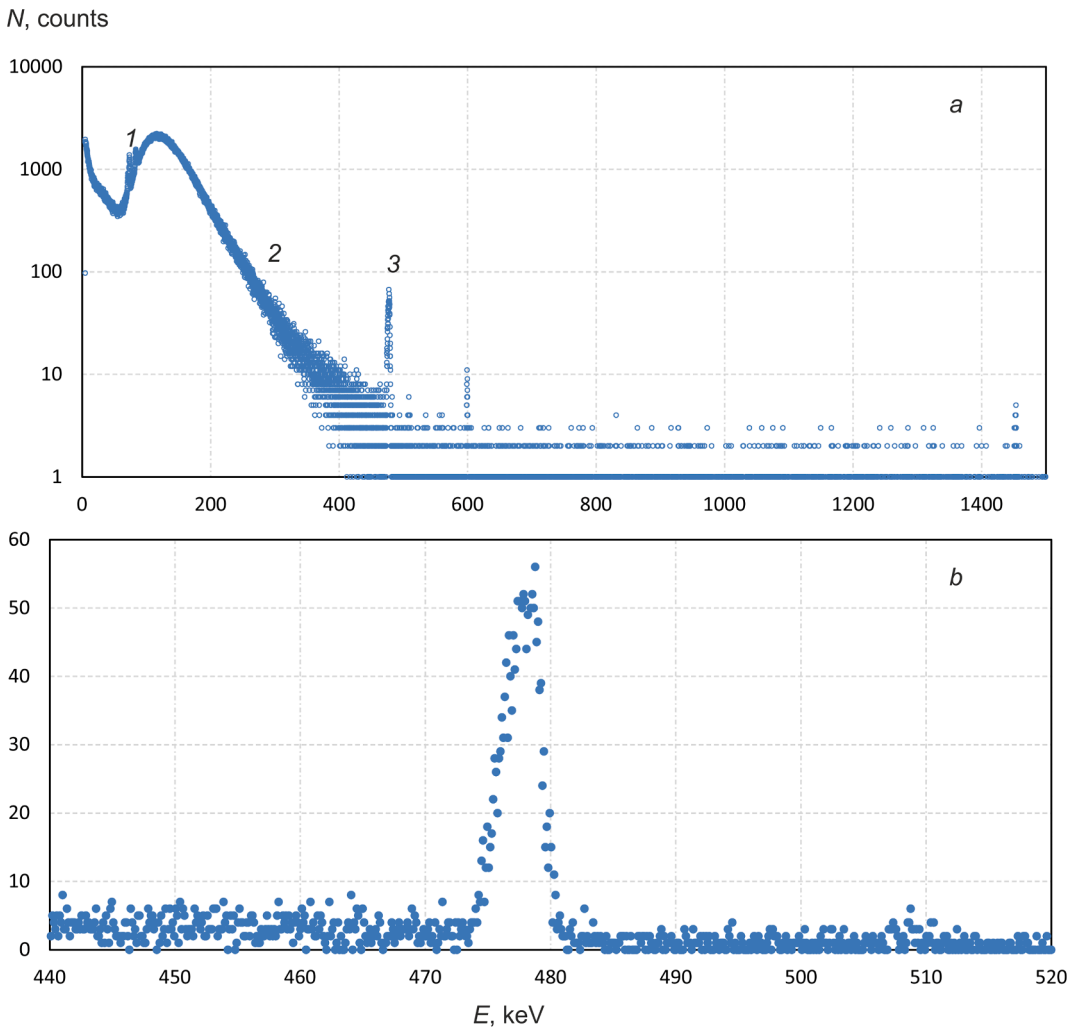

Fig. 4. The signal from HPGe γ-ray spectrometer when irradiating the thin lithium target: *1* – characteristic X-rays emitted by lead, *2* – bremsstrahlung of the accelerator, 3 – 478 keV photons emitted in the ^{7}Li(p,p'γ)^{7}Li reaction.

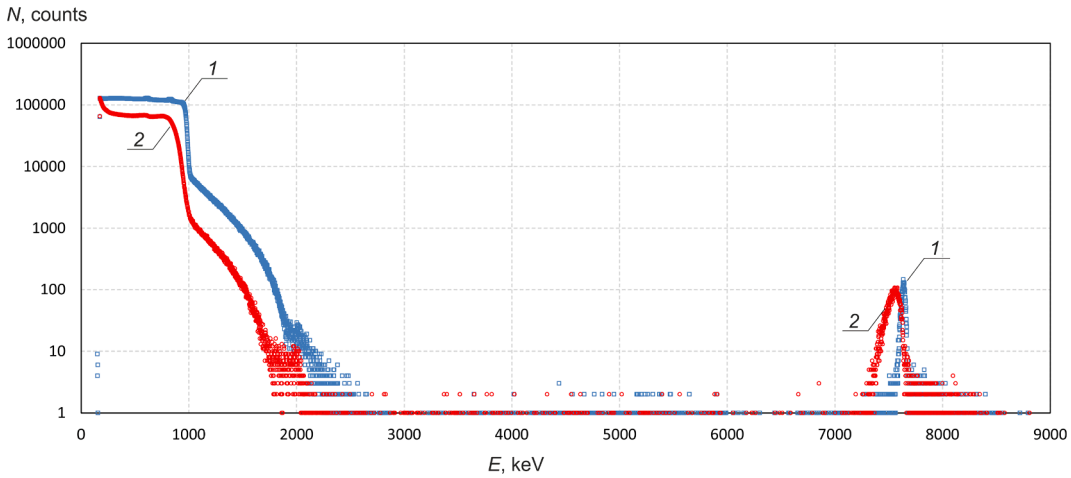

Fig. 5. The spectrum of charged particles detected by the α-spectrometer at the proton energy of 1 MeV: 1 – measured at the lithium thickness of 0.422 μm and presented in the article [21], 2 – measured to determine the thickness of the lithium layer.

1 ^{7}Li + d = n + ^{8}Be + 15.028 MeV
^{8}Be → 2 α + 0.094 MeV;
2 ^{7}Li + d = n + α + α + 15.121 MeV;
3 ^{7}Li + d = α + ^{5}He + 14.162 MeV
^{5}He → n + α + 0.957 MeV;
4 ^{6}Li + d = α + α + 22.38 MeV;
5 ^{6}Li + d = n + ^{7}Be + 3.385 MeV;
6 ^{6}Li + d = p + ^{7}Li + 5.028 MeV;

Table 1
The *G* values for two angles for the reactions at the used deuteron energies.

θ, °	E_d, keV	*G* ^{6}Li(d,α)^{4}He	^{6}Li(d,p)^{7}Li	^{6}Li(d,p)^{7}Li*	^{7}Li(d,α)^{5}He
135	333	1.0883	1.0687	1.0721	1.0993
	441	1.1018	1.0787	1.0826	1.1144
	547	1.1136	1.0872	1.0914	1.1275
	650	1.1240	1.0946	1.0991	1.1391
	760	1.1341	1.1018	1.1066	1.1504
	864	1.1431	1.1080	1.1130	1.1603
	962	1.1511	1.1133	1.1185	1.1690
	1064	1.1589	1.1186	1.1240	1.1776
	1170	1.1666	1.1237	1.1292	1.1861
	1270	1.1736	1.1282	1.1338	1.1937
	1372	1.1804	1.1326	1.1383	1.2011
	1473	1.1868	1.1366	1.1425	1.2081
	1573	1.1930	1.1405	1.1464	1.2148
	1674	1.1990	1.1442	1.1502	1.2213
	1776	1.2049	1.1477	1.1538	1.2276
	1877	1.2105	1.1511	1.1573	1.2336
	1977	1.2159	1.1543	1.1605	1.2394
	2078	1.2212	1.1574	1.1637	1.2450
	2179	1.2263	1.1604	1.1667	1.2505
168	329	1.1298	1.0995	1.1047	1.1471
	439	1.1512	1.1148	1.1208	1.1715
	545	1.1701	1.1281	1.1347	1.1930
	651	1.1871	1.1397	1.1469	1.2124
	756	1.2041	1.1511	1.1587	1.2317
	859	1.2193	1.1610	1.1691	1.249
	963	1.2329	1.1697	1.1782	1.2645
	1065	1.2466	1.1783	1.1871	1.2800
	1168	1.2603	1.1867	1.1958	1.2955
	1268	1.2727	1.1942	1.2036	1.3096
	1372	1.2850	1.2014	1.2111	1.3235
	1473	1.2969	1.2083	1.2183	1.3369
	1573	1.3083	1.2148	1.2250	1.3498
	1675	1.3196	1.2211	1.2315	1.3625
	1776	1.3307	1.2272	1.2378	1.3751
	1877	1.3415	1.2330	1.2438	1.3872
	1979	1.3520	1.2386	1.2495	1.3989
	2078	1.3624	1.2440	1.2550	1.4105
	2180	1.3726	1.2492	1.2603	1.4219

7 ^{6}Li + d = p + ^{7}Li* + 4.550 MeV;
8 ^{6}Li + d = t + p + α + 2.6 MeV;
9 ^{6}Li + d = t + ^{5}Li + 0.595 MeV
^{5}Li → α + p + 1.965 MeV;
10 ^{6}Li + d = ^{3}He+ ^{5}He + 0.840 MeV
^{5}He → n + α + 0.957 MeV.

In a number of reactions, the reaction products have low energy and cannot be identified in our study due to the presence of a much larger signal from backscattered deuterons. The α-spectrometer clearly allows identifying the products of reactions 2, 3, 4, 6, 7 and, therefore, measuring the cross-section of the ^{7}Li(d,nα)^{4}He, ^{7}Li(d,α)^{5}He, ^{6}Li(d,α)^{4}He, ^{6}Li(d,p)^{7}Li, and ^{6}Li(d,p)^{7}Li* reactions. A typical spectrum from the α-spectrometer is shown in Fig. 2.

4. Lithium layer thickness measurement

Let us determine the thickness of the lithium layer *l*. It was measured by new *in situ* method [17]. The method is based on comparing the yield of 478 keV photons in the ^{7}Li(p,p′γ)^{7}Li reaction when irradiating the investigated lithium layer and a thick one by protons. In this case a proton beam with the energy of 1.2 MeV was used.

A thick layer is a layer of lithium with the thickness greater than the length of the proton path in lithium up to the ^{7}Li(p,p′γ)^{7}Li reaction threshold which equals to 0.478 MeV. When selecting the lithium thickness, we used the expression for the proton energy loss rate *S* in lithium depending on its energy *E* [18]:

$$S = \frac{S_{low} \bullet S_{high}}{S_{low} + S_{high}} \text{eV}/(10^{15}\text{atoms}/cm^2),$$

where $S_{low} = 1{,}6\,E^{0{,}45}$, $S_{high} = \frac{725{,}6}{E}\ln(1 + \frac{3013}{E} + 0{,}04578\,E)$, *E* in keV. By means of this formula, we obtain that the proton projected range in lithium is 72 μm for 1.2 MeV proton and 17 μm for 0.478 MeV proton (note that proton total path length and the projected range practically do not differ). Consequently, at the initial proton energy of 1.2 MeV, photons are generated up to the depth of 55 μm from the lithium surface.

A 113 μm thick lithium layer was evaporated on the target, for which 320 mg of lithium were used (for weighing, an analytical balance OHAUS PX-84 (USA) was used, the minimum weighing limit is 200 mg, the accuracy is 0.1 mg). The target was irradiated with a proton beam, and the γ-ray spectrum was measured with a HPGe γ-ray spectrometer. The spectrum of γ-rays measured during 1507 s (live time 1470 s) at the proton beam current of 1.12 μA is shown in Fig. 3. The count rate of the 478 keV line is 16.08 count/s, per unit of current is 14.32 count/(s μA), integrated peak counts is 23642.

Then the lithium layer was washed off the target with water, and a thin layer of lithium (~6 mg, approximately 2 μm thick) was deposited onto the target. The target with the thin lithium layer was placed in the same position, and the γ-ray spectrum was measured with athe γ-ray spectrometer during 2102 s (live time 2059 s) at the proton beam current of 0.96 μA (Fig. 4). The count rate of the 478 keV line is 0.86 count/s, per unit of current is 0.89 count/(s μA), integrated peak counts is 1796.

The ratio of the emission intensity of 478 keV photons per unit current from the studied lithium layer and from the thick one is $A = 0.89/14.32 = 0.0625$, or 6.25 % with an accuracy of 3 % due to the statistical error. We found that the yield of 478 keV photons from the thin lithium target is 16 times less than from the thick one when irradiated with a proton beam with the energy of 1.2 MeV.

Previously we measured the yield of 478 keV photons from the thick lithium target [19], and found that at the energy of 1200.6 ± 1.2 keV it is equal to 1.76 ± 0.01 μC^{-1}, and at the energy of 1174.0 ± 1.4 keV it is equal to 1.61 ± 0.01 μC^{-1}, i.e., the photon yield dropped by 8.52 ± 0.8 % with a decrease in energy by 26.6 ± 0.14 keV. In other words, if the thickness of the lithium were such that a 1.2 MeV proton lost 26.6 keV as it passed through, then the yield of 478 keV photons from this layer of lithium would be 8.5 % of the yield from the thick target. In our case the yield from the measured lithium layer is 6.25 %, this means that the proton loses 19.5 ± 2 keV. Since the rate of deceleration of a 1.2 MeV proton according to the above formula [18] is equal to 10.66 keV/μm, we obtain the thickness of lithium equals 1.83 ± 0.2 μm. The low accuracy of determining the lithium thickness of 10 % is due to the fact that we subtracted two close values of the measured photon yield.

The accuracy of determining the thickness of lithium can be improved if we take not measured but calculated from the reaction cross-section presented in the article [19] values of the photon radiation intensity from the thick lithium target. Since the 478 keV line count rates on the thin and thick targets were measured in 25 keV steps, the count rate Y_j of γ-quanta from the thick target can be determined from the measured count rate Y_i from the thin target as $Y_j = \sum_{i=0}^{j} Y_i \frac{25}{S_i(x)}$, where the index *i* indicates the measurement number ($i = 0$ at 0.7 MeV, $i = 1$ at 0.725 MeV and so on in increments of 25 keV) and $S_i(x)$ is the value of the proton energy loss (in keV) in a lithium layer with the thickness *x*. The count rate from the thin lithium target is $Y_i = n\,x\,\sigma I/e$, where *x* is the thickness of lithium, *n* is the density of lithium atomic nuclei ($4.59 \cdot 10^{22}$ cm^{-3}), σ is the ^{7}Li(p,p'γ)^{7}Li reaction cross-section, *I* is the proton beam current, *e* is elementary charge. In the formula, the photon yield at the proton energy of 0.7 MeV is taken as a starting point, since the yield from the threshold at 0.478 up to 0.7 MeV can be neglected. In this case, we find that a decrease in the yield by 6.25 % occurs when the proton energy decreases by 19.3 ± 0.4 keV. Taking the value of the deceleration rate of a 1.2 MeV proton equal to 10.66 keV/μm and taking into account

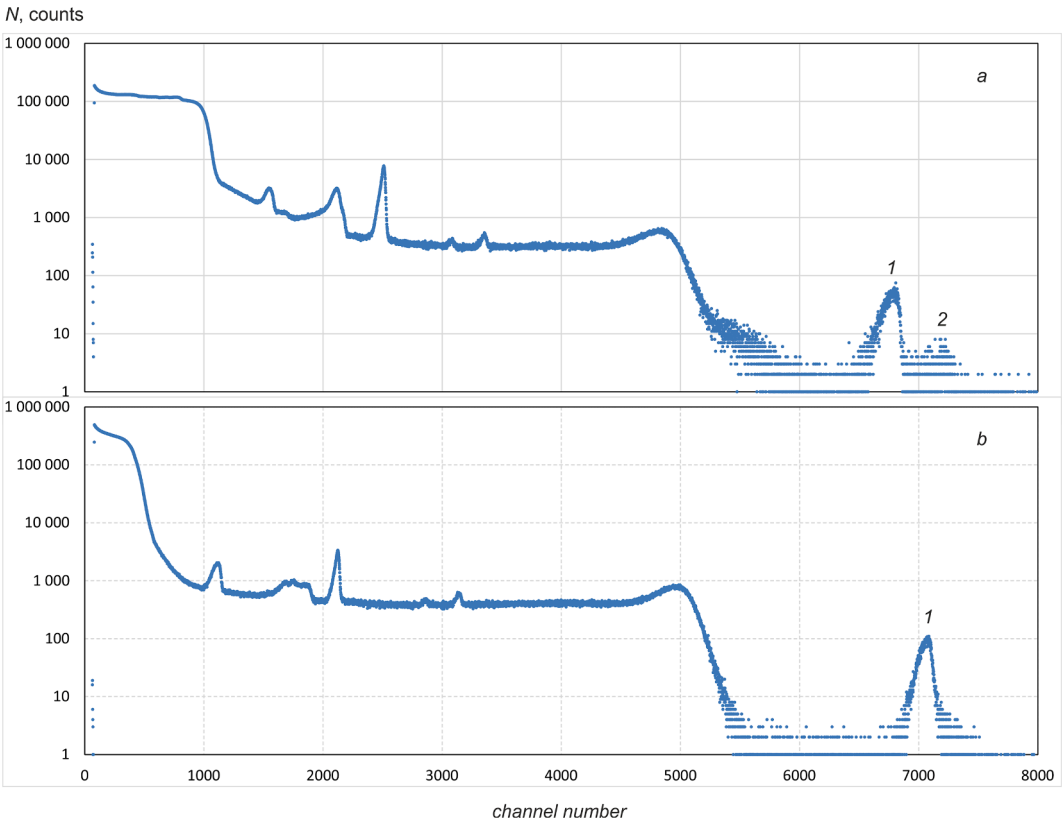

Fig. 6. The signal from the α-spectrometer at 1.8 MeV (*a*) and 0.9 MeV (*b*) deuteron beam: *1* – α-particles produced in the ^{6}Li(d,α)^{4}He reaction by deuterons with total energy, *2* – α-particles produced in the ^{6}Li(d,α)^{4}He reaction by deuterons with half the energy. The α-spectrometer is placed at the angle of 135°.

the statistical error in the yield ratio of 3 %, we obtain that the thickness of lithium is 1.81 ± 0.06 μm.

Previously we found that the lithium layer was covered with a layer containing atomic nuclei of carbon and oxygen due to the thermal evaporation of lithium in vacuum [20]. Using the backscattered protons energy analysis method we determined that the layer contains carbon and oxygen atomic nuclei in abundance of around 15 % and 40 % of the number of lithium atomic nuclei. Approximately the same content is obtained if we analyze the yield of the ^{12}C(d,p)^{13}C, ^{16}O(d,p)^{17}O и ^{16}O(d,α)^{14}N reactions. According to [18], the rate of proton deceleration on carbon atomic nuclei is 1.75 times greater than on lithium atomic nuclei, and oxygen is 2.17 times greater. The presence of carbon and oxygen in the lithium layer at concentrations of 15 % and 40 % leads to a 2-fold greater proton energy loss. This means that the average proton energy in the lithium layer will not be $E_{av} = 1200–19.3/2 = 1190.35$ keV, but $E_{av} = 1200–(19.3 \times 2)/2 = 1180.7$ keV. Due to this additional decrease in energy by 9.65 keV, the average deceleration rate increases by 0.6 % and the reaction cross section increases by 0.5 %. Taking these processes into account the thickness of the lithium layer decreases by 1.1 %, namely $l = 1.79 \pm 0.07$ μm. We will use this value of lithium thickness when determining the cross-sections of the nuclear reactions.

Additional confirmation of the correctness of determining the thickness of lithium was obtained by comparing the yield of the ^{7}Li(p,α)^{4}He reaction products which we measured earlier from a lithium layer with the thickness of 0.422 μm and published in [21] and measured now. To measure now we used the same target assembly with the α-spectrometer placed at the angle of 168°, but the α-spectrometer was placed at the greater distance – $r_2 = 712$ mm instead of $r_1 = 516$ mm. Spectra of charged particles detected by the α-spectrometer at the proton energy of 1 MeV are shown in Fig. 5. There is the signal of backscattered protons on the left (in the energy region up to 3 MeV) and the signal of α-particles and simultaneous registration of an α-particle and a proton on the right in the graph (in the energy region above 7.3 MeV).

The measurements were carried out at the same proton fluence, equal to 3.44 mC. When irradiating lithium layer with the thickness of 0.422 μm, total time $T_{total1} = 3908$ s, live time $T_{live1} = 3623$ s, and integrated peak counts of α-particles $Y_1 = 4536$ (Table 1 in [10]). When irradiating lithium, the thickness of which to determined, total time $T_{total2} = 3654$ s, live time $T_{live2} = 3501$ s, and integrated peak counts of α-particles $Y_2 = 10195$. We found the thickness of the lithium layer to be $l = 0.422 \times (Y_2/Y_1) \times (r_2/r_1)^2 \times (T_{total2}/T_{live2})/(T_{total1}/T_{live1}) = 0.422 \times 2.24 \times 1.9 \times 1.04/1.08 = 1.75$ μm. This lithium thickness value agrees well with that determined above.

5. Deuteron beam content

The beam of charged particles produced by the accelerator predominantly contains D^+ ions, but D_2^+ ions and D^0 neutrals are also present in the beam. D_2^- ions are generated in the ion source together with D^- ions; D^0 neutrals are formed in the gas stripper of the tandem accelerator due to the incomplete stripping of D^- ions into D^+ ions. D_2^+ ion and D^0 neutral interact with the lithium atomic nucleus as particles with half the energy of D^+ ion.

Fig. 6a shows that the energy spectrum of the ^{6}Li(d,α)^{4}He reaction products contains two peaks: the left one is caused by deuterons with the energy of 1.8 MeV, the right one is caused by deuterons with half the energy. The separation of the peaks is due to the fact that the higher the deuteron energy the lower the energy of the emitted back α-particle. At the same time, at the energy of 0.9 MeV, the peak caused by deuterons with half the energy is not visible (Fig. 6b). This is explained by the reaction cross-section: there is a maximum at the energy of 0.9 MeV and almost half as much at energies of 1.8 MeV and 0.45 MeV.

Let us determine the contribution of this component with half the

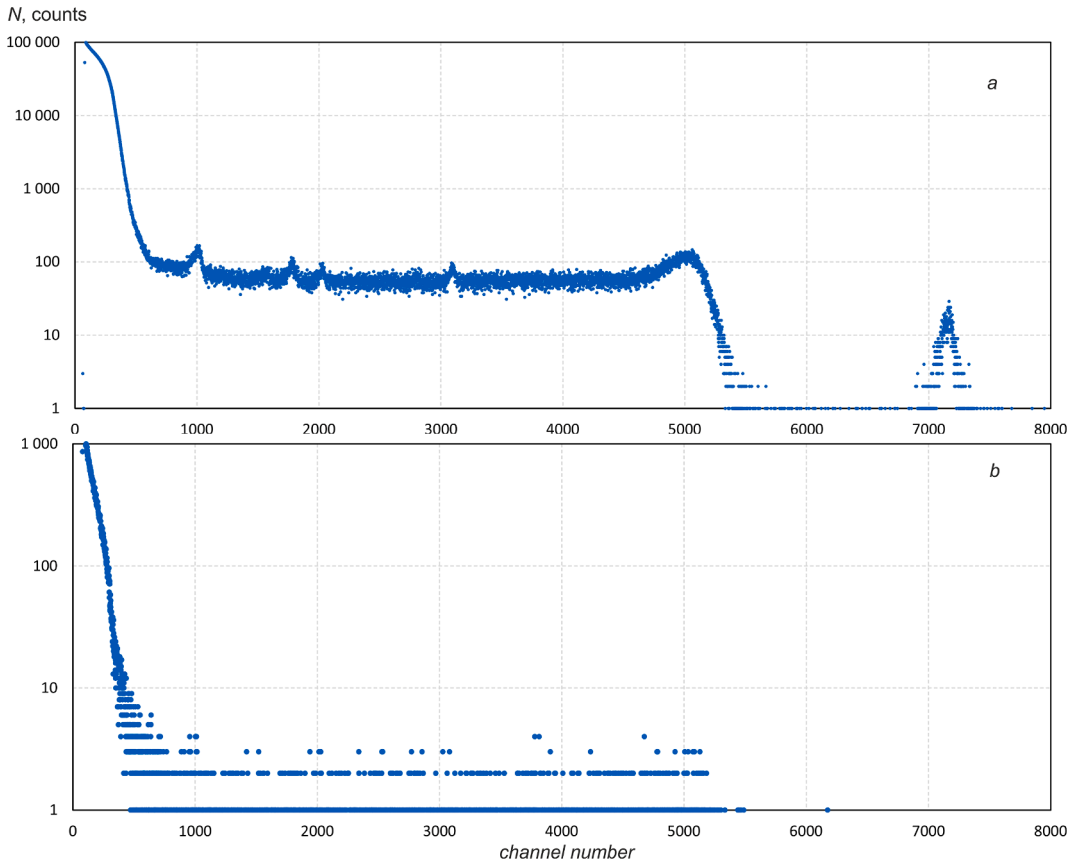

Fig. 7. The signal from the α-spectrometer: *a*) a deuteron beam with the energy of 0.7 MeV; the bending magnet is turned off, *b*) a deuteron beam with the energy of 1.4 MeV; the bending magnet is turned on. The α-spectrometer is placed at the angle of 135°.

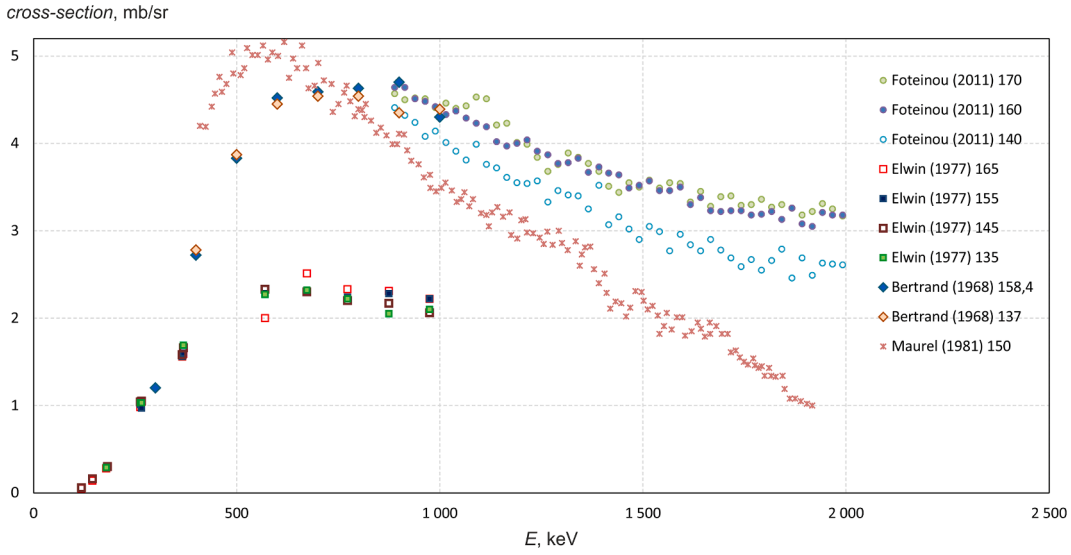

Fig. 8. The differential cross-sections of the ^{6}Li(d,α)^{4}He reaction data reported in the IBANDL database [23]. The legend indicates the authors, the year and the angle at which the measurements were taken.

energy. At the deuteron energy of 0.9 MeV (Fig. 6b), the α-particle peak *1* contains 11,439 events due to ions with total energy. At the deuteron energy of 1.8 MeV (Fig. 6a), the α-particle peak *2* contains 517 events due to half-energy ions. Considering that the fluence of the deuterium ion beam at the energy of 1.8 MeV was 1.06 times greater than at the energy of 0.9 MeV, we obtain the contribution of deuterons with half the energy equals 4 % of deuterons with full energy.

In order to determine which particles with half the energy interact with lithium atomic nuclei we turn on the bending magnet (*11* in Fig. 1): ions will be deflected in the magnetic field, and only neutrals will hit the lithium target. The α-spectrometer signals without the magnetic field and with the magnetic field are shown in Fig. 7. When the lithium target was irradiated with the ion beam, 2.7 10^{5} events were recorded by the α-spectrometer in channels from 1000 to 8000. When the lithium target

Table 2
Measured yield of α-particles or protons (integrated peak counts) Y of ^{6}Li(d,α)^{4}He, ^{6}Li(d,p)^{7}Li, ^{6}Li(d,p)^{7}Li*, ^{7}Li(d,α)^{5}He, and ^{7}Li(d,nα)^{4}He reactions at 135° and 168°: E – the average energy of a deuteron interacting with lithium atomic nuclei, ΔE – the standard deviation of E, T_{total} – total measurement time, T_{live} – live time measurement by α-spectrometer, Φ – D^{+} ion fluence.

E,	ΔE,	T_{total},	T_{live},	Φ,	Y, counts				
keV	keV	s	s	mC	^{6}Li(d,α)^{4}He	^{6}Li(d,p)^{7}Li	^{6}Li(d,p)^{7}Li*	^{7}Li(d,α)^{5}He	^{7}Li(d,nα)^{4}He
θ = 135°									
333	72	8711	8649	16.2	6775	4106	868	31,887	177,132
441	63	8922	8758	22.1	13,433	8140	2063	90,207	533,846
547	56	8942	8750	17.7	12,275	8361	2502	119,911	807,435
650	53	7583	7246	17.6	12,930	8795	2728	226,459	1,417,547
760	47	8798	8463	14.8	10,545	8182	2470	250,140	1,372,687
864	43	8868	8452	17.2	11,539	10,042	3417	257,906	1,553,223
962	41	8787	8463	12.4	7947	7310	2585	159,769	1,208,375
1064	38	8776	8448	12.1	7368	6931	3099	176,931	1,095,923
1170	37	12,762	12,204	19.8	11,274	11,386	4653	221,231	1,131,111
1270	34	9057	8744	15.7	8508	8762	3526	141,663	1,139,152
1372	32	9272	8871	15.2	7679	8236	3220	122,645	776,041
1473	31	9037	8684	13.3	6445	7099	2776	104,626	686,947
1573	29	7622	7244	13.8	6308	7215	3519	138,119	720,959
1674	28	7858	7467	15.1	6572	7906	3385	164,362	890,732
1776	27	8911	8445	18.3	7618	9351	3868	222,369	1,217,034
1877	26	8792	8354	17.1	6914	8416	3590	232,300	1,249,042
1977	25	8745	8330	16.4	6321	8226	2773	251,351	1,276,808
2078	24	8950	8519	17.1	6474	8126	3423	295,469	1,439,256
2179	23	9335	8881	18.0	6616	7687	3252	368,502	1,620,589
θ = 168°									
329	72	6671	6620	11.2	4338	2298	457	17,063	109,401
439	63	6125	5979	10.9	6410	3752	825	39,762	235,932
545	56	6144	5966	10.8	7960	4674	1084	73,817	433,888
651	51	6174	5972	10.3	8046	5403	1386	128,598	684,060
756	46	6645	6383	11.1	8623	5865	1316	172,364	918,449
859	43	6323	6052	11.2	8348	5790	1316	153,804	904,455
963	40	6286	5991	11.8	8280	5760	1336	157,723	1,013,899
1065	38	6296	6021	11.2	7343	5107	1503	176,425	905,837
1168	36	7392	7056	13.2	8417	6150	2089	155,178	732,673
1268	34	5427	5170	9.5	5838	4484	901	88,672	450,897
1372	32	6559	5972	11.5	6438	5570	1605	93,774	533,629
1473	31	6878	6666	12.6	7180	5670	1068	111,659	611,156
1573	29	6279	6004	11.2	6224	5153	1182	107,582	622,115
1675	28	6197	5923	11.5	5970	5075	1007	129,713	721,556
1776	27	6185	5912	11.2	5831	4555	1618	146,542	858,236
1877	26	6237	5963	11.4	5732	4566	1515	182,838	1,003,209
1979	25	6305	6033	11.6	5696	4608	1660	197,989	1,144,455
2078	24	6231	5975	11.2	5505	4554	2170	229,457	1,182,653
2180	24	6259	6005	11.1	5385	4232	2310	254,101	1,252,862

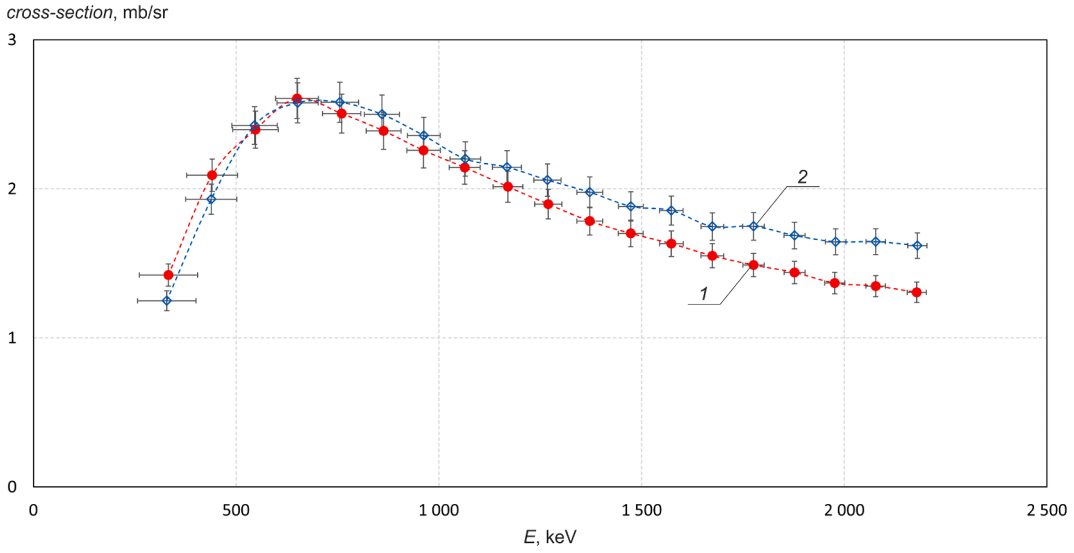

Fig. 9. The measured differential cross-section of the ^{6}Li(d,α)^{4}He reaction at 135° (*1*) and 168° (*2*).

Table 3
The differential cross-section of the ^{6}Li(d,α)^{4}He reaction at 135°: E – the deuteron energy, ΔE – the standard deviation of E, σ – the cross section, Δσ – the statistical variance of σ.

E, keV	ΔE, keV	σ, mb/sr	Δσ, mb/sr
333	72	1.42	0.07
441	63	2.09	0.11
547	56	2.40	0.12
650	53	2.61	0.13
760	47	2.51	0.13
864	43	2.39	0.12
962	41	2.26	0.12
1064	38	2.14	0.11
1170	37	2.01	0.10
1270	34	1.90	0.10
1372	32	1.78	0.09
1473	31	1.70	0.09
1573	29	1.63	0.09
1674	28	1.55	0.08
1776	27	1.49	0.08
1877	26	1.44	0.08
1977	25	1.37	0.07
2078	24	1.35	0.07
2179	23	1.31	0.07

Table 4
The differential cross-section of the ^{6}Li(d,α)^{4}He reaction at 168°: E – the deuteron energy, ΔE – the standard deviation of E, σ – the cross section, Δσ – the statistical variance of σ.

E, keV	ΔE, keV	σ, mb/sr	Δσ, mb/sr
329	72	1.25	0.07
439	63	1.93	0.10
545	56	2.43	0.13
651	51	2.58	0.13
756	46	2.58	0.13
859	43	2.50	0.13
963	40	2.36	0.12
1065	38	2.20	0.12
1168	36	2.15	0.11
1268	34	2.06	0.11
1372	32	1.98	0.10
1473	31	1.88	0.10
1573	29	1.85	0.10
1675	28	1.75	0.09
1776	27	1.75	0.09
1877	26	1.69	0.09
1979	25	1.64	0.09
2078	24	1.65	0.09
2180	24	1.62	0.09

was irradiated with neutrals, 1.6 10^3 events were recorded in these channels. Since the fluence of the deuteron beam with the turned on bending magnet was 3 times greater, we conclude that the contribution of neutrals to the ion beam is 0.2 %. This value is less than 4 % defined as the contribution of deuterons with half the energy. Consequently, deuterons with half the energy are obtained from D_2^+ ions. Since each D_2^+ ion produces two deuterons, and each of them interacts with lithium atomic nuclei, we obtain the following composition of the beam irradiating the lithium target: 98 % of D^+ ions, 2 % of D_2^+ ions, the contribution of neutrals can be neglected.

6. Measuring reaction cross-sections

The cross-sections of the reactions ^{7}Li(d,nα)^{4}He, ^{7}Li(d,α)^{5}He, ^{6}Li(d,α)^{4}He, ^{6}Li(d,p)^{7}Li, and ^{6}Li(d,p)^{7}Li* were measured as follows. A thin layer of lithium was irradiated with a deuteron beam, and an α-spectrometer measured α-particles and protons emitted at a certain solid angle. The differential cross-section of the reaction in the laboratory coordinates dσ/dΩ was found from the formula:

$$\frac{d\sigma}{d\Omega} = \frac{eY}{Nknl\Phi\,\Omega_{lab}},$$

where e is elementary charge, Y the experimental yield of α-particles or protons (integrated peak counts), N the number of measured charged particles in a reaction ($N = 2$ in the ^{7}Li(d,nα)^{4}He and ^{6}Li(d,α)^{4}He reactions; $N = 1$ in other reactions), k the efficiency of registration of α-particles by the spectrometer ($k = 1$ with an accuracy of 3 %), n the density of Li nuclei ($n = 4.251{\cdot}10^{22}$ cm^{-3} for ^{7}Li with the accuracy of 0.1 %; $n = 0.345{\cdot}10^{22}$ cm^{-3} for ^{6}Li with the accuracy of 1 %), l the lithium thickness ($l = 1.79$ μm with the accuracy of 4 %), Φ D^+ fluence, Ω_{lab} the solid angle ($\Omega_{lab} = 3.84{\cdot}10^{-5}$ at the angle of 135°; $\Omega_{lab} = 3.95{\cdot}10^{-5}$ at the angle of 168°).

The relationship of the differential cross section in the center of mass system $d\sigma_{c.m.}/d\Omega_{c.m.}$ and in the laboratory coordinates dσ/dΩ is given by the formula [22]:

$$\frac{d\sigma_{c.m.}}{d\Omega_{c.m.}} = \frac{|1+\beta cos\theta|}{(1+\beta^2+2\beta cos\theta)^{\frac{3}{2}}}\frac{d\sigma}{d\Omega},$$

where $\beta = \sqrt{\frac{\widetilde{m_d M}}{M_B M} \bullet \frac{T_M}{T_M+Q}}$ and $T_M = E_d\frac{M}{(m_d+M)}$, M, $M^{\sim}$ are the masses of decay particles, in this case the mass of proton or α-particle, m_d is the deuteron mass, M_B the mass of the target particle, in this case mass of lithium-6 or lithium-7, θ the particle detection angle in the laboratory coordinates, in this case 135° or 168°, Q the reaction energy yield, E_d the kinetic energy of incident deuteron. For convenience we introduce the coefficient connecting the coordinate systems G:

$$G = \frac{|1+\beta\cos\theta|}{(1+\beta^2+2\beta\cos\theta)^{\frac{3}{2}}}.$$

The calculated G values for two angles for the reactions at the used deuteron beam energies are given in Table 1.

If the radiation is isotropic in the center of mass system, then the cross section of the reaction σ will be defined as:

$$\sigma = 4\,\pi\,G\,d\sigma/d\Omega$$

7. ^{6}Li(d,α)^{4}He reaction

The ^{6}Li(d,α)^{4}He reaction produces two α-particles with the same high energy, and, therefore, α-particles are easily identified in the measured energy spectrum of charged particles (see *10* in Fig. 2). At low deuteron energies, this peak of α-particles is far enough away from the rest of the recorded events, and it easy to count the integrated peak. At high deuteron energies, double events from other reactions and products of the ^{6}Li(d,α)^{4}He reaction from deuterons with half the energy appear in the region of this peak. However, these contributions are small and easy to estimate.

Fig. 8 shows the differential cross-section of the ^{6}Li(d,α)^{4}He reaction data reported in the IBANDL database (Ion Beam Analysis Nuclear Data Library, International Atomic Energy Agency) [23]. One can see that the data in two groups differ by a factor of two. The cross section of the ^{6}Li(d,α)^{4}He reaction σ is presented in the ENDF/B-VIII.0 Evaluated Nuclear Reaction Data Library [24] (this cross-section is identical in the TENDL-2019 database [25], there is no this cross-section in the Japanese Evaluated Nuclear Data Library JENDL [26]); it is shown below in Fig. 12 in comparison with the results obtained.

The measured yields of α-particles or protons (integrated peak counts) Y of the ^{6}Li(d,α)^{4}He, ^{6}Li(d,p)^{7}Li, ^{6}Li(d,p)^{7}Li*, ^{7}Li(d,α)^{5}He, and ^{7}Li(d,nα)^{4}He reactions at 135° and 168° are presented in Table 2. The measurements were carried out 100 keV deuteron beam energy steps. The measured energy of the deuteron beam differed from the set energy by no more than 5 keV; energy stability was 1–2 keV, maximum 4 keV. When a deuteron passes through the lithium layer, the deuteron loses

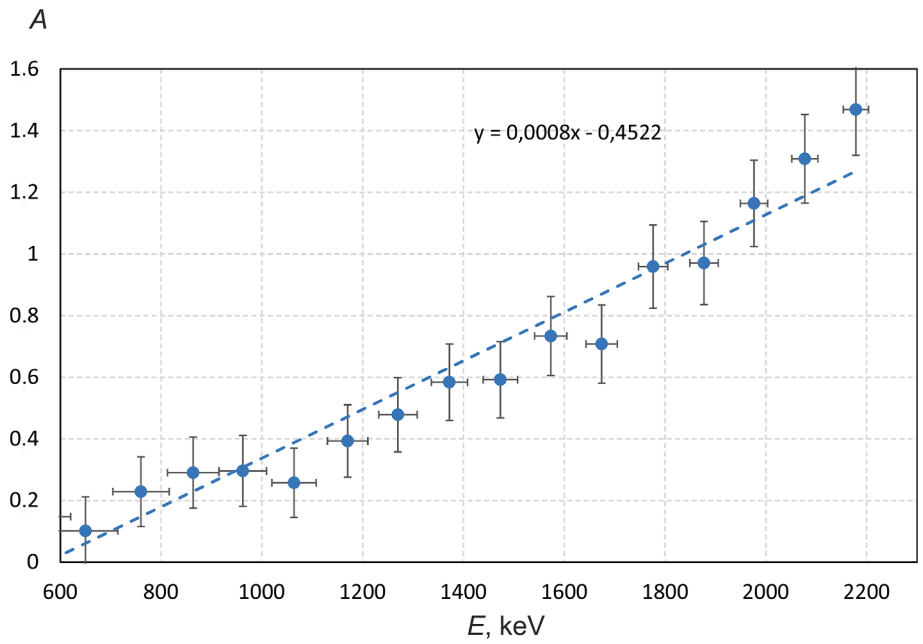

Fig. 10. The dependence of the coefficient *A* on the energy *E*.

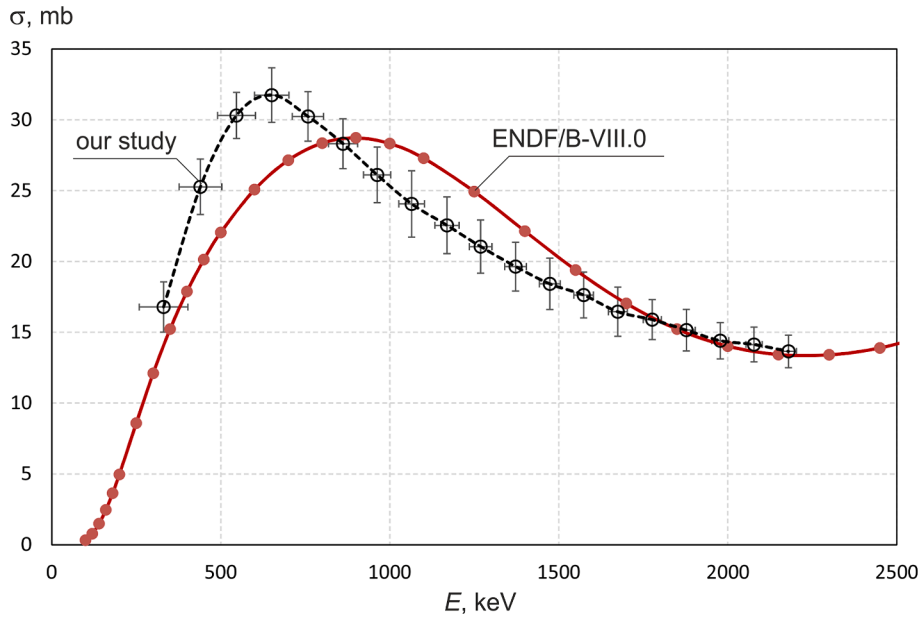

Fig. 11. The measured cross-section of the ^{6}Li(d,α)^{4}He reaction and presented in the ENDF/B-VIII.0 Evaluated Nuclear Reaction Data Library [24].

energy from 43 keV at the energy of 2.2 MeV to 142 keV at the energy of 0.4 MeV (taking into account the presence of carbon and oxygen in the lithium layer). Table 2 gives exactly this deuteron energy, namely the average energy of deuterons in the lithium layer, not the energy of the incident deuteron at the lithium surface.

The data obtained make it possible to determine the differential cross-section of the ^{6}Li(d,α)^{4}He reaction; it is given in Fig. 9 and in Tables 3 and 4. The accuracy of cross-section measurement is determined by the accuracy of lithium thickness determination (4 %), the accuracy of efficiency of charge particle registration determination (3 %), the accuracy of density of Li nuclei determination (1 %), and standard error (1–1.5 %); in total it is 5.3 %.

As is known, the differential cross section of the ^{6}Li(d,α)^{4}He reaction in the center of mass system is described by the formula:

$$\frac{d\sigma(\theta)}{d\Omega}_{c.m.} = \frac{d\sigma(90^{\circ})}{d\Omega}_{c.m.}(1 + A(E)\cos^2\theta + \cdots)$$

In our energy range we neglect higher order terms [27] and use following angular dependence: $1 + A(E)\ cos^2\theta$. Since the measurements were carried out at two angles, we determine the coefficient $A(E)$. The dependence of coefficient A on energy is shown in Fig. 10. The trend line is given by the following expression: $A(E) = 0.8\ E$ (MeV) – 0.4522.

If we integrate over all angles we get the total cross section as a function of energy:

$$\sigma(\theta)_{c.m.} = \frac{d\sigma(90^{\circ})}{d\Omega}_{c.m.}\int_0^{2\pi} d\varphi \int_0^{\pi}(1 + A(E)\cos^2\theta)\sin\theta d\theta =$$

Finally:

Table 5
The cross-section of the ^{6}Li(d,α)^{4}He reaction: E – the deuteron energy, ΔE – the standard deviation of E, σ – the cross section, Δσ – the statistical variance of σ.

E, keV	ΔE, keV	σ, mb	Δσ, mb
331	73	16.8	1.8
440	64	25.3	2.0
546	56	30.3	1.6
651	51	31.7	1.9
758	47	30.2	1.7
861	44	28.3	1.8
963	40	26.1	2.0
1065	38	24.1	2.3
1169	36	22.6	2.0
1269	34	21.0	1.9
1372	32	19.6	1.7
1473	31	18.4	1.8
1573	29	17.6	1.6
1675	28	16.4	1.7
1776	27	15.9	1.4
1877	26	15.2	1.5
1978	25	14.4	1.3
2078	24	14.1	1.2
2180	24	13.6	1.1

$$\sigma(\theta)_{c.m.} = 4\pi \frac{d\sigma(90^{\circ})}{d\Omega}_{c.m.} \left(1 + \frac{A(E)}{3}\right)$$

Then we obtain the reaction cross section by integrating the yield over the angle; it is given in Fig. 11 and in Table 5.

8. ^{6}Li(d,p)^{7}Li and ^{6}Li(d,p)^{7}Li* reactions

The ^{6}Li(d,p)^{7}Li and ^{6}Li(d,p)^{7}Li* reactions produces protons detected by the α-spectrometer (see *6* and *7* in Fig. 2). These peaks are clearly identified on the plateau of α-particles from the ^{7}Li(d,nα)^{4}He reaction (see *8* in Fig. 2).

Fig. 12 shows the differential cross-sections of the ^{6}Li(d,α)^{4}He and ^{6}Li(d,p)^{7}Li* reactions data reported in the IBANDL database [23]. There are two groups of values. The cross-sections of the ^{6}Li(d,α)^{4}He and ^{6}Li(d,p)^{7}Li* reactions σ are presented in the ENDF/B-VIII.0 [24].

The measured yields of protons (integrated peak counts) Y of the ^{6}Li(d,p)^{7}Li and ^{6}Li(d,p)^{7}Li* reactions at 135° and 168° are presented in Table 2. The data obtained make it possible to determine the differential cross-section of the ^{6}Li(d,p)^{7}Li and ^{6}Li(d,p)^{7}Li* reactions; it is given in Fig. 13 and in Tables 6 and 7. The accuracy of cross-section measurement is determined by the accuracy of lithium thickness determination (4 %), the accuracy of efficiency of charge particle registration determination (3 %), the accuracy of density of Li nuclei determination (1 %). The main measurement error is determined by the standard error of the mean value of plateau of α-particles from the ^{7}Li(d,nα)^{4}He reaction

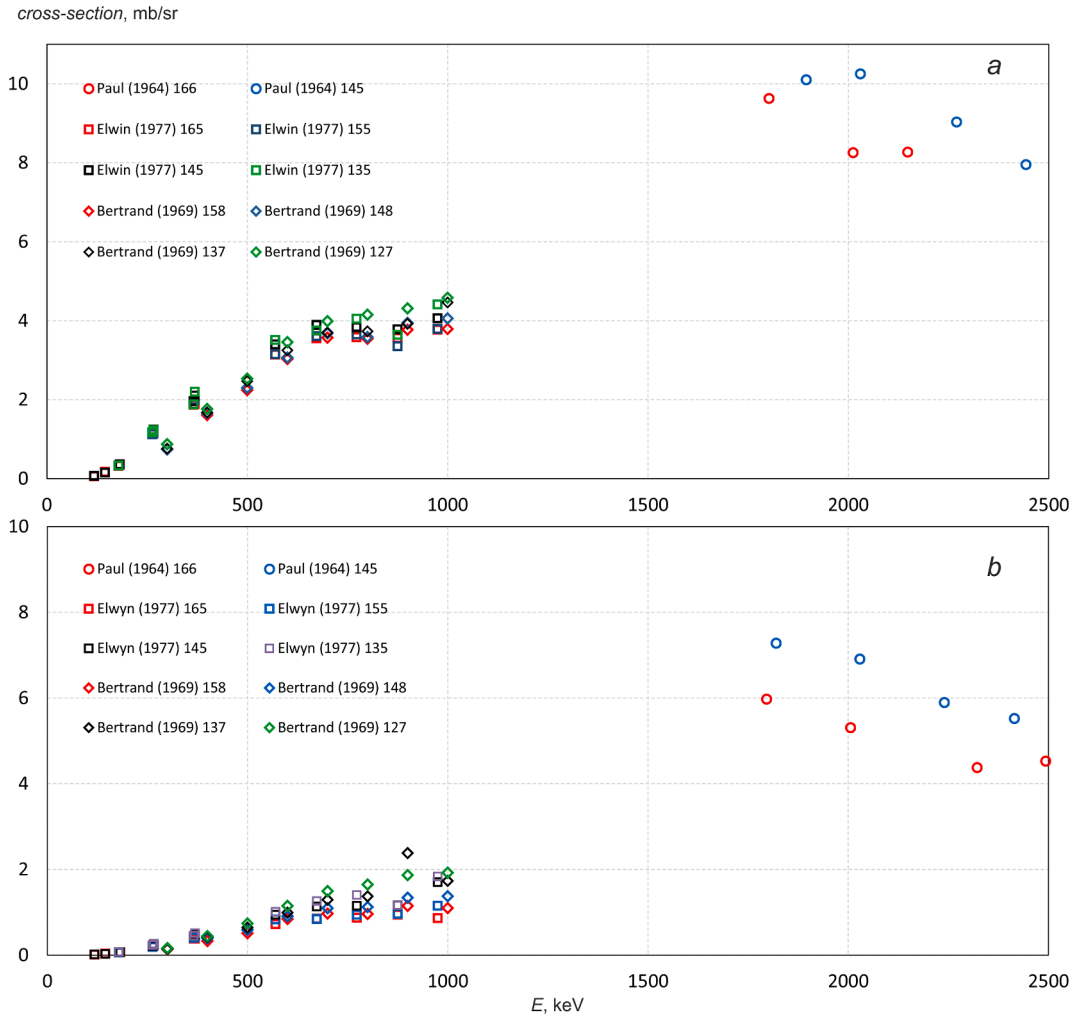

Fig. 12. The differential cross-section of the ^{6}Li(d,p)^{7}Li (a) and ^{6}Li(d,p)^{7}Li* (b) reactions [23]. The legend indicates the authors, the year and the angle at which the measurements were taken.

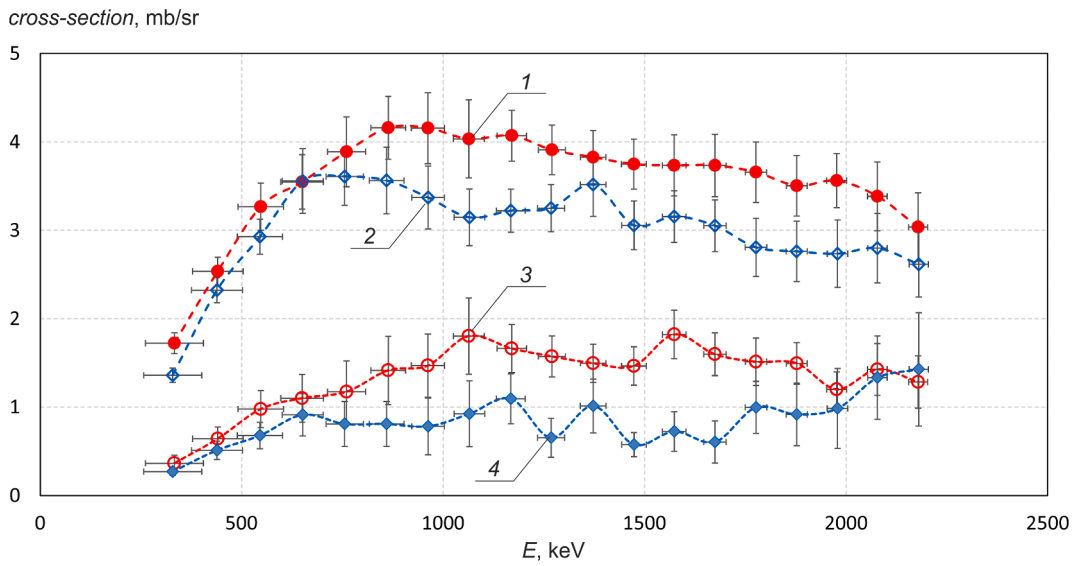

Fig. 13. The measured differential cross-sections of the ^{6}Li(d,p)^{7}Li reaction at 135° (*1*) and 168° (*2*), the ^{6}Li(d,p)^{7}Li*reaction at 135° (*3*) and 168° (*4*).

Table 6
The differential cross-section of the ^{6}Li(d,p)^{7}Li and ^{6}Li(d,p)^{7}Li* reactions at 135°: *E* – the deuteron energy, Δ*E* – the standard deviation of *E*, σ – the cross section, Δσ – the statistical variance of σ.

E, keV	Δ*E*, keV	Δσ, mb/sr	Δσ, mb/sr	Δσ, mb/sr	Δσ, mb/sr
		^{6}Li(d,p)^{7}Li reaction		^{6}Li(d,p)^{7}Li*reaction	
333	72	1.72	0.12	0.36	0.09
441	63	2.53	0.16	0.64	0.13
547	56	3.27	0.27	0.98	0.21
650	53	3.55	0.31	1.10	0.27
760	47	3.89	0.39	1.17	0.35
864	43	4.16	0.36	1.42	0.39
962	41	4.15	0.40	1.47	0.36
1064	38	4.03	0.44	1.80	0.43
1170	37	4.07	0.29	1.66	0.27
1270	34	3.91	0.28	1.57	0.23
1372	32	3.83	0.30	1.50	0.22
1473	31	3.75	0.28	1.47	0.22
1573	29	3.73	0.35	1.82	0.27
1674	28	3.73	0.35	1.60	0.24
1776	27	3.66	0.34	1.51	0.27
1877	26	3.50	0.34	1.49	0.23
1977	25	3.56	0.31	1.20	0.20
2078	24	3.38	0.39	1.43	0.29
2179	23	3.03	0.39	1.28	0.30

Table 7
The differential cross-section of the ^{6}Li(d,p)^{7}Li and ^{6}Li(d,p)^{7}Li* reactions at 168°: *E* – the deuteron energy, Δ*E* – the standard deviation of *E*, σ – the cross section, Δσ – the statistical variance of σ.

E, keV	Δ*E*, keV	Δσ, mb/sr	Δσ, mb/sr	Δσ, mb/sr	Δσ, mb/sr
		^{6}Li(d,p)^{7}Li reaction		^{6}Li(d,p)^{7}Li*reaction	
329	72	1.36	0.08	0.27	0.04
439	63	2.32	0.14	0.51	0.10
545	56	2.93	0.20	0.68	0.15
651	51	3.56	0.37	0.91	0.24
756	46	3.61	0.33	0.81	0.25
859	43	3.56	0.38	0.81	0.25
963	40	3.37	0.36	0.78	0.32
1065	38	3.15	0.32	0.92	0.37
1168	36	3.22	0.24	1.09	0.28
1268	34	3.25	0.27	0.65	0.22
1372	32	3.52	0.36	1.01	0.30
1473	31	3.05	0.28	0.58	0.14
1573	29	3.15	0.29	0.72	0.22
1675	28	3.05	0.29	0.61	0.24
1776	27	2.81	0.33	1.00	0.29
1877	26	2.76	0.34	0.92	0.35
1979	25	2.73	0.38	0.98	0.45
2078	24	2.80	0.39	1.33	0.47
2180	24	2.61	0.37	1.43	0.64

determination relative to the ^{6}Li(d,p)^{7}Li and ^{6}Li(d,p)^{7}Li* reactions distributions fittings: 5–10 % for ^{6}Li(d,p)^{7}Li and 15–40 % for ^{6}Li(d,p)^{7}Li*. The total accuracy of the cross-section measurement is 7–12 % for ^{6}Li(d,p)^{7}Li and 15–40 % for ^{6}Li(d,p)^{7}Li*.

9. ^{7}Li(d,α)^{5}He reaction

The ^{7}Li(d,α)^{5}He reaction produces α-particles detected by the α-spectrometer (see *9* in Fig. 2). This peak is clearly identified. The resulting ^{5}He atomic nucleus almost instantly decays into a neutron and an α-particle. The energy spectrum of these α-particles is wider: from 3 MeV to 7 MeV.

The measured yields of α-particles *Y* of the ^{7}Li(d,α)^{5}He reaction at 135° and 168° are presented in Table 2. The data obtained make it possible to determine the differential cross-section of the ^{7}Li(d,α)^{5}He reaction; it is given in Fig. 14 and in Tables 8 and 9. When calculating the cross-section we subtracted the contribution of half-energy deuterons to the signal assuming the D_2^+ ion current to be equal to 2 % of the D^+ ion current. The accuracy of cross-section measurement is determined by the accuracy of lithium thickness determination (4 %), the accuracy of efficiency of charge particle registration determination (3 %), the accuracy of density of Li nuclei determination (1 %), standard error (1 %), and uncertainty in the contribution of half-energy deuterons (0–2 %); in total it is 6 %.

10. ^{7}Li(d,nα)^{4}He reaction

There are no data on the ^{7}Li(d,nα)^{4}He reaction in the literature or databases.

The ^{7}Li(d,nα)^{4}He reaction produces two α-particles detected by the α-spectrometer (see *8* in Fig. 2). Fig. 15 shows the signal of the α-spectrometer at 0.6 MeV deuteron beam to explain how the number of reaction events is calculated. The kinematics of the reaction is such that the energy of the α-particle is greater than a certain one, depending on the angle and the energy of the deuteron. So for the deuteron energy of 0.6 MeV and the angle of 135° this α-particle energy is equal to 551 keV.

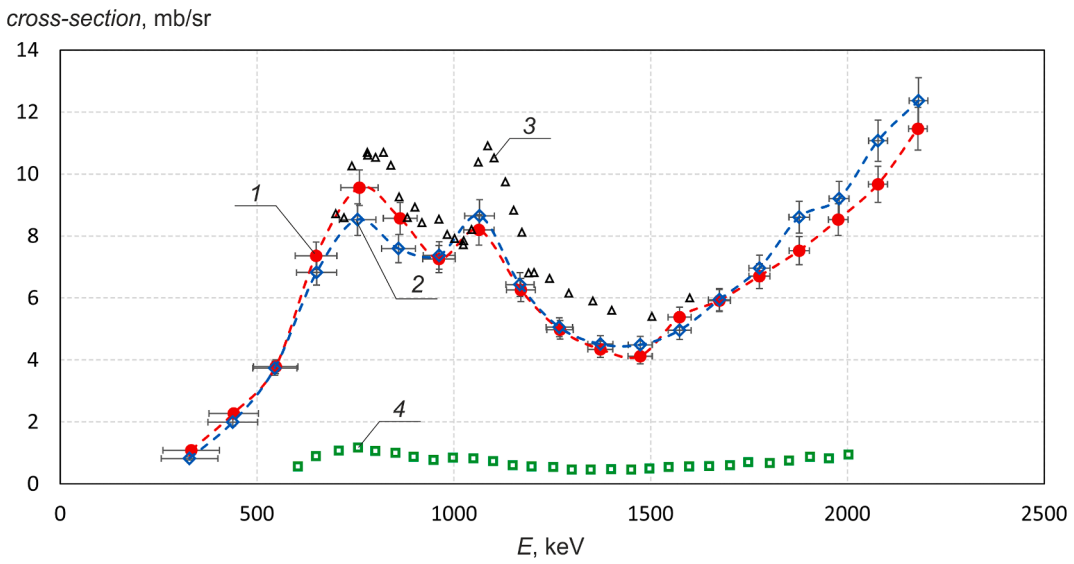

Fig. 14. The measured differential cross-section of the ^{7}Li(d,α)^{5}He reaction at 135° (1) and 168° (2). For comparison data from the ENDF/B-VIII.0 [24] is provided: 3 – Delbrouck-Habaru (1969) 154°, 4 – Friendland (1971) 90°.

Table 8
The differential cross-section of the ^{7}Li(d,α)^{5}He reaction at 135°: E – the deuteron energy, ΔE – the standard deviation of E, σ – the cross section, Δσ – the statistical variance of σ.

E, keV	ΔE, keV	σ, mb/sr	Δσ, mb/sr
333	72	1.09	0.07
441	63	2.27	0.14
547	56	3.78	0.23
650	53	7.36	0.44
760	47	9.56	0.57
864	43	8.57	0.51
962	41	7.26	0.44
1064	38	8.20	0.49
1170	37	6.26	0.38
1270	34	4.97	0.30
1372	32	4.34	0.26
1473	31	4.12	0.25
1573	29	5.38	0.32
1674	28	5.91	0.35
1776	27	6.70	0.40
1877	26	7.53	0.45
1977	25	8.53	0.51
2078	24	9.67	0.58
2179	23	11.46	0.69

Table 9
The differential cross-section of the ^{7}Li(d,α)^{5}He reaction at 168°: E – the deuteron energy, ΔE – the standard deviation of E, σ – the cross section, Δσ – the statistical variance of σ.

E, keV	ΔE, keV	σ, mb/sr	Δσ, mb/sr
329	72	0.82	0.05
439	63	1.99	0.12
545	56	3.73	0.22
651	51	6.82	0.41
756	46	8.53	0.51
859	43	7.59	0.46
963	40	7.37	0.44
1065	38	8.65	0.52
1168	36	6.43	0.39
1268	34	5.06	0.30
1372	32	4.51	0.27
1473	31	4.49	0.27
1573	29	4.95	0.30
1675	28	5.94	0.36
1776	27	6.96	0.42
1877	26	8.61	0.52
1979	25	9.21	0.55
2078	24	11.07	0.66
2180	24	12.37	0.74

Particles with such energy are registered by the α-spectrometer channel $N_m = 308$. In the region from the channel N_m to the region in which the contribution of backscattered deuterons can be neglected we draw a smooth curve (*7* in Fig. 15) that approximately describes the contribution of the ^{7}Li(d,nα)^{4}He reaction α-particles. Then we sum up all the events under the curve *7* and all the events to the right of the curve *7*; we get Y_s. We define the yield of α-particles Y of the ^{7}Li(d,nα)^{4}He reaction as $Y = Y_s - Y_1 - Y_2 - Y_3 - Y_4 - Y_5 - 2\,Y_6$, where Y_i is the number of counts in peaks *1–6* (the majority of values are given in Table 2).

The measured yields of α-particles Y of the ^{7}Li(d,nα)^{4}He reaction at 135° and 168° are presented in Table 2. The data obtained make it possible to determine the differential cross-section of the ^{7}Li(d,nα)^{4}He reaction; it is given in Fig. 16 and in Tables 10 and 11. When calculating the cross-section we subtracted the contribution of half-energy deuterons to the signal assuming the D_2^+ ion current to be equal to 2 % of the D^+ ion current. The accuracy of cross-section measurement is determined by the accuracy of lithium thickness determination (4 %), the accuracy of efficiency of charge particle registration determination (3 %), the accuracy of density of Li nuclei determination (1 %), uncertainty in the contribution of half-energy deuterons (0–2 %), and uncertainty drawing a curve depicting the contribution of the ^{7}Li(d,nα)^{4}He reaction at low energies (≈ 2 %); in total it is 7 %.

11. Conclusion

The interaction of deuterons with lithium is characterized by a large number of nuclear reactions with the generation of neutrons, α-particles, protons, tritium, helium-3, lithium-7, and beryllium-7. However, the reliable data on the cross-section of these nuclear reactions are extremely scarce, and for some reactions the data are absent. In this study, the ^{6}Li(d,α)^{4}He, ^{6}Li(d,p)^{7}Li, ^{6}Li(d,p)^{7}Li*, ^{7}Li(d,α)^{5}He, and ^{7}Li(d,nα)^{4}He reactions cross-sections at the deuteron energies from 0.3 MeV to 2.2 MeV was measured with high precision.

Funding

This work was supported by the Russian Science Foundation (grant number 19-72-30005).

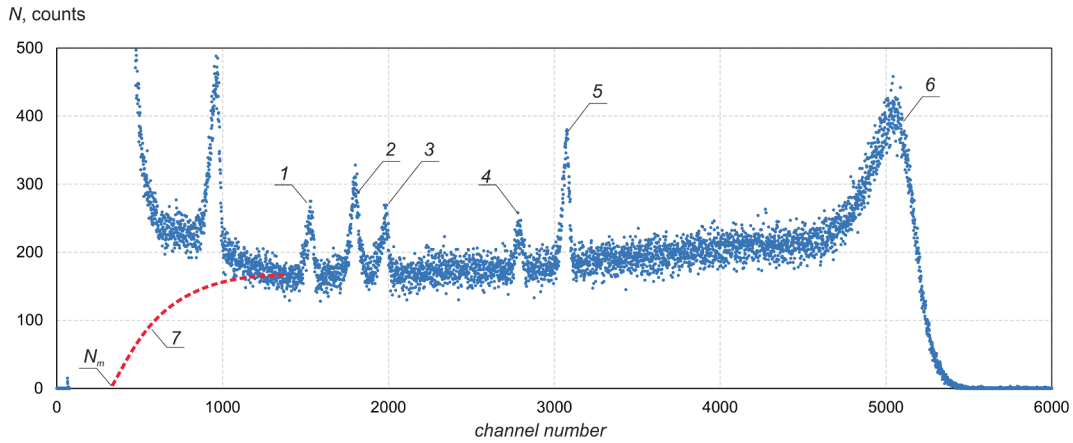

Fig. 15. The signal from the α-spectrometer at 0.6 MeV deuteron beam at 135°: *1* – $^{16}O(d,p_0)^{17}O$ reaction protons, *2* – $^{16}O(d,\alpha)^{14}N$ reaction α-particles, *3* – $^{12}C(d,p_0)^{13}C$ reaction protons, *4* – $^{6}Li(d,p_1)^{7}Li^*$ reaction protons, *5* – $^{6}Li(d,p_0)^{7}Li$ reaction protons, *6* – $^{7}Li(d,\alpha)^{5}He$ reaction α-particles, *7* – line depicting the $^{7}Li(d,n\alpha)^{4}He$ reaction α-particles contribution, N_m – the spectrometer channel corresponding to the minimum possible energy of the $^{7}Li(d,n\alpha)^{4}He$ reaction α-particles.

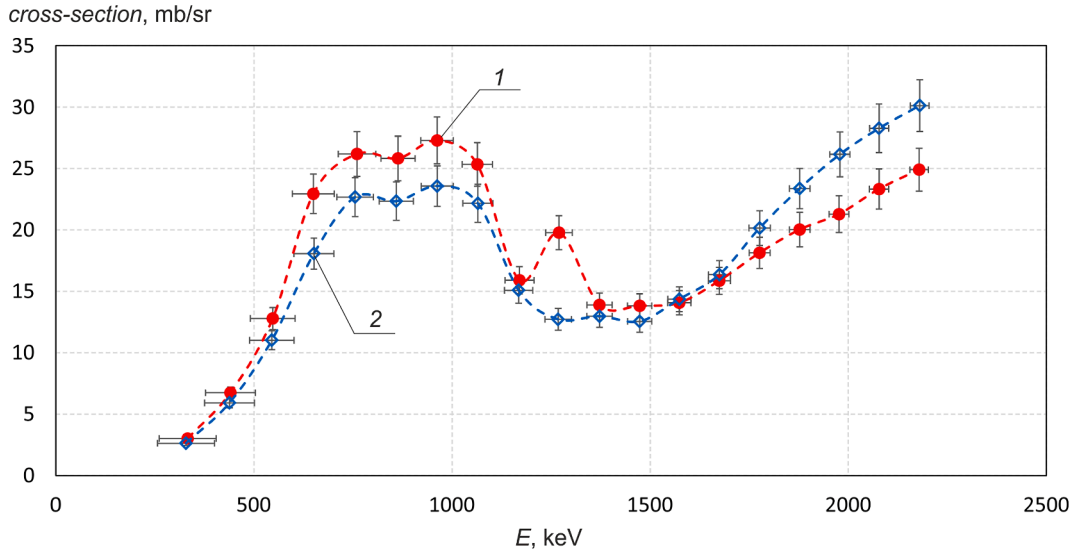

Fig. 16. The measured differential cross-section of the $^{7}Li(d,n\alpha)^{4}He$ reaction at 135° (*1*) and 168° (*2*).

Table 10
The differential cross-section of the $^{7}Li(d,n\alpha)^{4}He$ reaction at 135°: *E* – the deuteron energy, Δ*E* – the standard deviation of *E*, σ – the cross section, Δσ – the statistical variance of σ.

E, keV	Δ*E*, keV	σ, mb/sr	Δσ, mb/sr
333	72	3.0	0.2
441	63	6.7	0.5
547	56	12.8	0.9
650	53	22.9	1.6
760	47	26.2	1.8
864	43	25.8	1.8
962	41	27.3	1.9
1064	38	25.3	1.8
1170	37	15.9	1.1
1270	34	19.8	1.4
1372	32	13.9	1.0
1473	31	13.8	1.0
1573	29	14.1	1.0
1674	28	15.8	1.1
1776	27	18.1	1.3
1877	26	20.0	1.4
1977	25	21.3	1.5
2078	24	23.3	1.6
2179	23	24.9	1.7

Table 11
The differential cross-section of the $^{7}Li(d,n\alpha)^{4}He$ reaction at 168°: *E* – the deuteron energy, Δ*E* – the standard deviation of *E*, σ – the cross section, Δσ – the statistical variance of σ.

E, keV	Δ*E*, keV	σ, mb/sr	Δσ, mb/sr
329	72	2.6	0.2
439	63	5.9	0.4
545	56	11.0	0.8
651	51	18.1	1.3
756	46	22.7	1.6
859	43	22.3	1.6
963	40	23.6	1.6
1065	38	22.2	1.6
1168	36	15.1	1.1
1268	34	12.7	0.9
1372	32	13.0	0.9
1473	31	12.5	0.9
1573	29	14.4	1.0
1675	28	16.4	1.1
1776	27	20.2	1.4
1877	26	23.4	1.6
1979	25	26.2	1.8
2078	24	28.3	2.0
2180	24	30.1	2.1

CRediT authorship contribution statement

Sergey Taskaev: Conceptualization, Supervision, Writing – review & editing. **Marina Bikchurina:** Investigation, Formal analysis. **Timofey Bykov:** Software. **Dmitrii Kasatov:** Formal analysis. **Iaroslav Kolesnikov:** Investigation. **Georgii Ostreinov:** Investigation, Writing – original draft. **Sergey Savinov:** Validation. **Evgeniia Sokolova:** Investigation.

Declaration of competing interest

The authors declare that they have no known competing financial interests or personal relationships that could have appeared to influence the work reported in this paper.

References

[1] S. Taskaev, Accelerator based epithermal neutron source, Phys. Part. Nucl. 46 (2015) 956–990, https://doi.org/10.1134/S1063779615060064.

[2] Tables of Physical Constants, Handbook. I.K. Kikoin Edition, AtomIzdat, Moscow (1976).

[3] A.J. Elwin, R.E. Holland, C.N. Davids, L. Meyer-Schtzmeister, J.E. Monahan, F. P. Mooring, W. Ray Jr., Absolute cross sections for deuteron-induced reactions on ^{6}Li at energies below 1 MeV, Phys. Rev C 16 (1977) 1744–1756, https://doi.org/10.1103/PhysRevC.16.1744.

[4] P. Paul, K.P. Lieb, The excited state at 25 MeV in Be^{8}, Nucl. Phys. 53 (1964) 465–476, https://doi.org/10.1016/0029-5582(64)90626-1.

[5] F. Bertrand, G. Grenier, J. Pornet, Study of the reactions ^{6}Li(pα)^{3}He, ^{6}Li(dα)^{4}He, ^{6}Li(dp$_0$)^{7}Li and ^{6}Li(dp$_1$)^{7}Li* from 300 keV to 1000 keV, Rept. Centre d'Etudes Nucleaires, Saclay Reports (1968) No.3428.

[6] Cai Dunjiu, Zhou Enchen, Jiang Chenglie, Cross section measurements of Li-6(d,α) He-4, 1985 (unpublished).

[7] J.M. Delbrouck-Habaru, P.D. Dumont, M. Huez, G. Robaye, L. Winand, Etude de la Section Efficace Differentielle a 154° des Reactions ^{6}Li(d,α)^{4}He et ^{7}Li(d.α)^{5}He dans Une Gamme d'Energie Incidente Variant de 500 a 1500 keV, Jour. Bull. Soc. Roy. Sci. Liege 38 (1969) 240 (1969).

[8] V. Foteinou, A. Lagoyannis, M. Kokkoris, G. Provatas, T. Konstantinopoulos, P. Misaelides, S. Harissopulos, Cross section measurements of the ^{6}Li(d,α$_0$)^{4}He reaction, Nucl. Instrum. Meth. B 269 (2011) 2990–2993, https://doi.org/10.1016/j.nimb.2011.04.058.

[9] B. Maurel, G. Amsel, D. Dieumegard, Microanalysis of fluorine by nuclear reactions: II. ^{19}F + d reactions, Nucl. Instrum. Meth. Phys. Res. 191 (1981) 349–356, https://doi.org/10.1016/0029-554X(81)91028-4.

[10] G. Bruno, J. Decharge, A. Perrin, G. Surget, C. Thibault, Distributions angulaires des réactions ^{6}Li(d,α)^{4}He, ^{6}Li(d, p$_0$)7Li, 6Li(d, p^{1})7Li* 0.47 MeV, J. Phys. France 27 (1966) 517–520, https://doi.org/10.1051/jphys:01966002709-10051700.

[11] W. Whaling, T.W. Bonner, Disintegration of Li^{6} by deuterons, J. Phys. Rev. 79 (1950) 258, https://doi.org/10.1103/PhysRev.79.258.

[12] F. Hirst, I. Johnstone, M.J. Poole, LXXXV. The d-^{6}Li reactions, The London, Edinburgh, and Dublin Philos. Mag. J. Sci. 45 (366) (1954) 762–766, https://doi.org/10.1080/14786440708520486.

[13] S. Taskaev, E. Berendeev, M. Bikchurina, T. Bykov, D. Kasatov, I. Kolesnikov, A. Koshkarev, A. Makarov, G. Ostreinov, V. Porosev, S. Savinov, I. Shchudlo, E. Sokolova, I. Sorokin, T. Sycheva, G. Verkhovod, Neutron source based on vacuum insulated tandem accelerator and lithium target, Biology 10 (2021) 350, https://doi.org/10.3390/biology10050350.

[14] S. Taskaev, Accelerator-based Neutron Source VITA, FizMatLit, Moscow, 2024.

[15] Handbook of Stable Isotope Analytical Techniques. Volume II (2009) 1123-1321, https://doi.org/10.1016/B978-0-444-51115-7.00028-0.

[16] K. Lieberman, G.J. Alexander, J.A. Sechzer, Stable isotopes of lithium: dissimilar biochemical and behavioral effects, Experientia 42 (1986) 985–987, https://doi.org/10.1007/BF01940701.

[17] D. Kasatov, Ia. Kolesnikov, A. Koshkarev, A. Makarov, E. Sokolova, I. Shchudlo, S. Taskaev, Method for in situ measuring the thickness of a lithium layer, J. Instrum. 15 (2020) P10006, https://doi.org/10.1088/1748-0221/15/10/P10006.

[18] H. Andersen, J. Ziegler, Hydrogen Stopping Powers and Ranges in all Elements. Volume 3 of the Stopping and Ranges of Ions in Matter, Pergamon Press Inc., 1977.

[19] S. Taskaev, T. Bykov, D. Kasatov, Ia. Kolesnikov, A. Koshkarev, A. Makarov, S. Savinov, I. Shchudlo, E. Sokolova, Measurement of the ^{7}Li(p, p'γ)7Li reaction cross-section and 478 keV photon yield from a thick lithium target at proton energies from 0.65 MeV to 2.225 MeV, Nucl. Instrum. Meth. Phys. Res. B 502 (2021) 85–94, https://doi.org/10.1016/j.nimb.2021.06.010.

[20] M. Bikchurina, T. Bykov, E. Byambatseren, I. Ibrahem, D. Kasatov, Ia. Kolesnikov, V. Konovalova, A. Koshkarev, A. Makarov, G. Ostreinov, S. Savinov, E. Sokolova, I. Sorokin, I. Shchudlo, T. Sycheva, G. Verkhovod, S. Taskaev, High flux neutron source for various applications, J. Neutron Res. 24 (2022) 273–279, https://doi.org/10.3233/JNR-220020.

[21] S. Taskaev, M. Bikchurina, T. Bykov, D. Kasatov, Ia. Kolesnikov, A. Makarov, G. Ostreinov, S. Savinov, E. Sokolova, Cross-section measurement for the ^{7}Li (p,α)^{4}He reaction at proton energies 0.6 - 2 MeV, Nucl. Instrum. Meth. Phys. Res. B 525 (2022) 55–61, https://doi.org/10.1016/j.nimb.2022.06.010.

[22] Yu. Shirokov, N. Yudin, Nuclear Physics, MIR Publishers, Moscow, 1982.

[23] https://www-nds.iaea.org/exfor/ibandl.htm.

[24] https://www.nndc.bnl.gov/endf-b8.0/.

[25] https://tendl.web.psi.ch/tendl_2019/tendl2019.html.

[26] https://wwwndc.jaea.go.jp/jendl/jendl.html.

[27] R. Resnick, D.R. Inglis, Theory of the lithium two-alpha reactions. II. Angular distribution of Li^{6}(d,α)α, Phys. Rev. 76 (1949) 1318–1323, https://doi.org/10.1103/PhysRev.76.1318.